Available online at www.sciencedirect.com
SCIENCE DIRECT®
Journal of Crystal Growth 292 (2006) 221–226
JOURNAL OF CRYSTAL GROWTH
www.elsevier.com/locate/jcrysgro

Role of excited nitrogen species in the growth of GaN by RF–MBE

T. Kikuchi[a], A.S. Somintac[a], O. Ariyada[b], M. Wada[a], T. Ohachi[a,*]

[a]Department of Electrical Engineering, Doshisha University, 1-3 Miyakodani tatara, Kyotanabe, Kyoto 610-0321, Japan
[b]Arios Inc. 3-2-20 Musashino Akishima, Tokyo 196-0021, Japan

Available online 14 June 2006

Abstract

Optical emission spectroscopy (OES) was used with the combinatorial growth method to investigate the behavior of excited nitrogen species in the growth of gallium nitride (GaN) using radio-frequency molecular beam epitaxy (RF–MBE). To determine the amounts of each excited nitrogen species in the nitrogen plasma, the integrated OES intensity (IOI) method was proposed. The IOI measurements revealed the following: more nitrogen ions (N_2^+) were produced at the lower inlet pressure of nitrogen, the productivity of nitrogen atoms (N) and excited nitrogen atoms (N^*) had an optimum value at some inlet pressure, whereas the productivity of excited nitrogen molecules (N_2^*) saturated as the inlet pressure increased. The combination of the IOI measurement and the combinatorial growth of GaN showed that not only N and N^*, but also the long-lifetime $A^3\Sigma_u^+$ state of N_2^* contributed to GaN growth using RF–MBE.

PACS: 52.70.Kz; 81.05.Ea; 81.15.Hi; 82.33.Xj

Keywords: A1. Optical emission spectroscopy; A3. Combinatorial growth; A3. Radio-frequency molecular beam epitaxy; B1. Nitrides; B2. Semiconducting III–V materials

1. Introduction

Polytypism (zincblende (cubic) and würtzite (hexagonal)) group-III nitrides, including AlN, GaN, InN (aluminum nitride, gallium nitride, and indium nitride) and their alloys, are promising candidates for high-temperature electronic and UV/blue optoelectronic devices due to their wide direct-energy band gap. Molecular beam epitaxy (MBE) is a common growth technique for device fabrication of compound semiconductors because MBE allows deposition at low substrate temperature and precise control of both the interface smoothness and the composition of alloy crystals. Moreover, the use of source materials is more economical with MBE compared to metal-organic chemical vapor deposition (MOCVD). Since nitrogen molecules are inert and have a strong N–N bond, they do not chemisorb on the surface of group-III nitrides. Therefore, plasma discharges are employed to produce excited nitrogen species such as nitrogen atoms (N), electrically excited nitrogen atoms (N^*), electrically excited nitrogen molecules (N_2^*) and nitrogen ions (N_2^+). Various techniques of plasma discharge including radio-frequency (RF) [1–4], microwave [5–7], electron cyclotron resonance of microwave plasma (μ-ECR) [1,8,9], and DC plasma [10] have been proposed in MBE growth. Of these methods, the RF plasma method is commonly used for the MBE-growth of group III-nitride because RF plasma produces less N_2^+ and more N and N^* compared to μ-ECR [1,11]. Hughes et al. [11] demonstrated a comparative GaN growth using RF and μ-ECR discharge. They concluded that h-GaN grown by using an RF discharge is superior to that grown by using an μ-ECR in the viewpoint of the growth rate, optical property. Nowadays, a growth rate of h-GaN exceeding 2.0 μm/h has been reported for hexagonal GaN growth with an RF source [12]. However, the effects of nitrogen discharge by RF plasma on the growth mechanism of group III-nitride in RF–MBE is not fully understood yet.

In this paper, we propose a method for determining the amounts of excited nitrogen species in RF–MBE by using optical emission spectroscopy (OES). This method is used to determine the dependency of the population of excited

*Corresponding author. Tel.: +81 774 65 6329; fax: +81 774 65 6811.
E-mail address: tohachi@mail.doshisha.ac.jp (T. Ohachi).

0022-0248/$ - see front matter © 2006 Elsevier B.V. All rights reserved.
doi:10.1016/j.jcrysgro.2006.04.019

species on the pressure of inlet nitrogen gas from an RF plasma source. Through combinatorial growth of h-GaN using RF–MBE, it will be revealed that $N_2^*(A^3\Sigma_u^+)$ contributes to the growth mechanism in RF–MBE for group-III nitrides.

2. Experimental procedure

2.1. Plasma diagnosis and epitaxial growth

All h-GaN growth and plasma diagnoses were performed using an MBE system (Oxford Instrument V.G. 80 H) equipped with an RF plasma source (Arios IRFS).

2.1.1. For plasma diagnosis

The RF source consisted of 3 parts shown in Fig. 1: part I, discharge of nitrogen in the discharge tube; part II, orifice design; and part III, flight stage of neutral and charged species. For this combination of both lower vacuum technique of RF plasma and ultrahigh vacuum technique of MBE, the orifice design of the discharge tube and the exhaust velocity are crucial for RF–MBE. The orifice is 0.5-mm thick and has 373 holes with 0.2-mm hole diameter. The calculated effective exhaust velocity is 625 L/s using 2 turbomolecular pumps. In this article, we focus on the discharge of nitrogen (part I in Fig. 1). The plasma diagnosis was done using OES measurements with a Peltier-cooled charge-coupled detector (CCD) (Hamamatsu Photonics PMA-11) through an optical window. PMA-11 was done with the standard wavelength and sensitivity correction from the National Institute of Standards and Technology by Hamamatsu Photonics. The nitrogen gas (99.99999%) was input into the discharge tube and monitored with a pressure gauge, as depicted in Fig. 1.

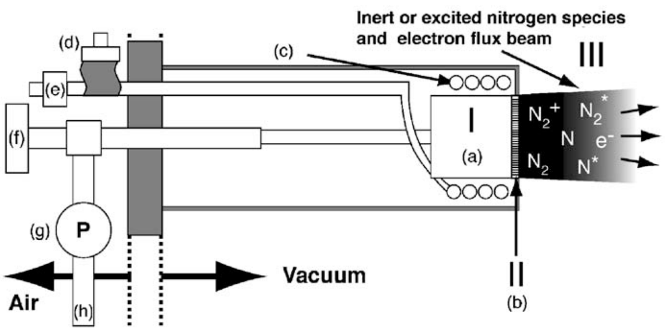

Fig. 1. Schematic setup of the RF source used in the experiments: (a) discharge tube made of pyrolitic boron nitride (PBN), (b) orifice made of PBN. The orifice has 373 holes 0.5-mm long with 0.2-mm diameter to confine the outlet excited nitrogen species, (c) RF inductive coil with 10.5 turns and water cooling, (d) connector for RF power supply. This connector is connected to an RF matching box, (e) connector to waterfeed line, (f) optical window for OES measurement, (g) pressure gauge for monitoring 'inlet pressure' of nitrogen gas, (h) feed line of nitrogen gas. Parts I–III are the places of the production of the excited spaces, the filtering the exciting and charged species, and the control of the flow of the excited and charged species, respectively.

2.1.2. For epitaxial growth

The substrate temperature was monitored using a thermocouple, and calibrated to both the formation temperature of Al/Si eutectics (577 °C) [13] and the transition temperature of 1100 K for the reflection high-energy electron diffraction (RHEED) reconstruction from (7×7) to (1×1) [14,15]. The Ga source (99.99999%) was loaded in a conventional Knudsen-effusion cell.

Three-inch Si (1 1 1) on-axis substrates were used for the substrate of h-GaN growth. Si (1 1 1) substrate was dipped into 5% HF (volume %) for several minutes, and then rinsed with deionized water. After the substrates were loaded into the MBE system, they were heated up to 650 °C for 30 min to remove the surface hydrogen termination. The RHEED pattern showed (7×7) reconstruction and did not indicate the unintentional formation of SiC on the Si (1 1 1) surface. Before h-GaN growth, a low temperature buffer (LTB) layer of GaN was directly deposited on Si (1 1 1) at 400 °C. Following LTB deposition, the substrate temperature was elevated to 700 °C and the bulk of h-GaN growth was then performed for 1 h under various inlet pressures of nitrogen gas (20–450 Pa). The Ga flux was carefully maintained at 1.07×10^{-6} Pa (BEP). The substrate was not rotated throughout the h-GaN growth, which is known as the combinatorial growth method. The growth chamber during h-GaN growth was kept below about 10^{-3} Pa. A focused ion beam (FIB) was used for obtaining cross-sectional images of the h-GaN layer to measure the thicknesses of the h-GaN epilayer.

2.2. Integrated OES intensity (IOI)

OES is a way to determine the plasma composition. Fig. 2a shows the typical spectrum of nitrogen plasma using an RF source. The peaks for the N (747 nm) and for N^* (822, 868, 906, 920 and 940 nm) are seen in the 700–950 nm range [16]. On the contrary, the spectrum of a molecular state instead shows a band like that for N_2^* in Fig. 2b due to the accumulation of vibration and rotation energy in molecular species. As shown in Fig. 2b, 'bandhead' is the wavelength for the peak point and 'bandtail' is the wavelength for the extinction point of the spectrum. Ideally, the shape of the bandhead is an abrupt rise at the higher wavelength, however, in practice, the shape of the bandhead is round, such as that in Fig. 2b. This is due to the lack of resolution for wavelength and sensitivity. The emission of '2nd-positive series of N_2' transitions from $C^3\Pi_u$ to $B^3\Pi_g$ (bandheads: 316, 337, 357, and 380 nm) and the '1st-negative series of N_2^+' transitions from $B^2\Sigma_u^+$ to $X^2\Sigma_g^+$ (bandheads: 391 and 428 nm) within the range of 300-500 nm are assigned [17]. The '1st-positive series of N_2' transitions from $B^3\Pi_g$ to $A^3\Pi_g$ is the most prominent emission in the region around 500 nm. This broad emission region is involved with the recombination between N, N^* and the third body, such as N_2 and the PBN (pyrolytic boron nitride) wall of a discharge tube. In an OES measurement, we measured the spontaneous emission

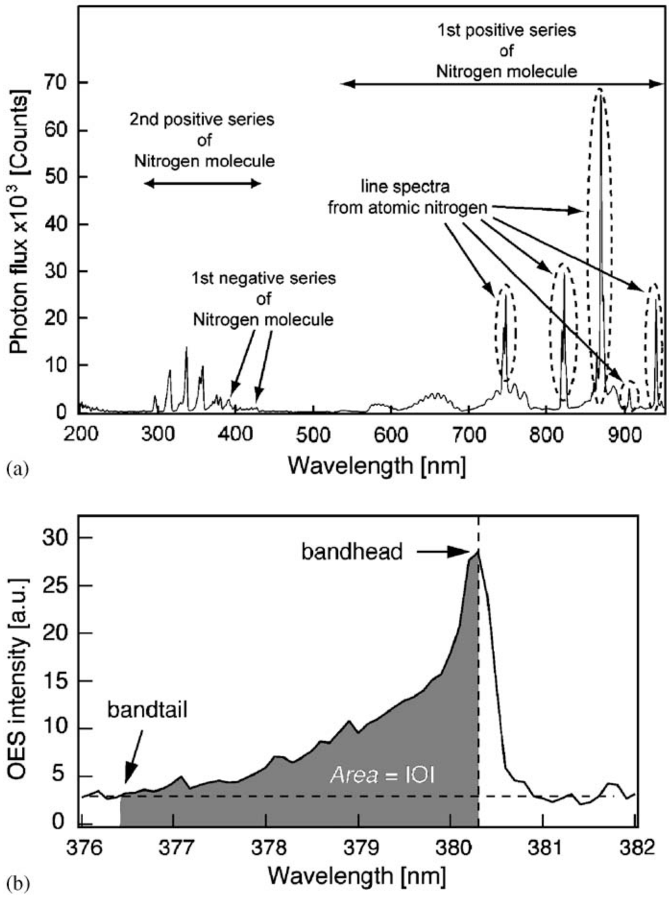

Fig. 2. Nitrogen spectra: (a) results of an OES measurement in 'bright mode discharge' typically observed using our RF source, (b) a part of the band spectrum from the 2nd positive series of N_2^* between 376 and 382 nm. The definition of bandhead and bandtail is shown.

caused by transition of particles from the excited state to a stable state. The optical intensity caused by the spontaneous emission, according to the transition of excited atoms, is

$$I = N^* Ah\nu, \tag{1}$$

where N^* is the number density of excited atoms of frequency ν, A is the Einstein A coefficient and h is Planck's constant. From Eq. (1), the intensity of optical emission (i.e., the intensity of spectra) is proportional to the number density of excited atoms. As mentiond above, the spectrum caused by the transition of excited niteogen molecules is band-like due to the accumulation of vibration and rotation energy in molecular species. To quantify the density of N_2^*, we used the following 1st order approximation

$$N_2^* \propto \sum_{\text{bandtail}}^{\text{bandhead}} I. \tag{2}$$

The integrated intensity of OES spectra refers to a summation of photons from band or line spectra. As mentioned above, the resolution problems should also be taken into account. For example, the integrated OES intensity (IOI) of the 380-nm peak, corresponding to a part of the 2nd-positive series of N_2^*, is the area colored gray in Fig. 2b. The IOI provides the relative density of the species in nitrogen plasma in accordance with their band or line emission. To determine the particle composition in the plasma discharge, the Ratio of the following equation is defined.

$$\text{Ratio} = \frac{\sum_{\text{bandtail}}^{\text{bandhead}} I}{\int I \, d\lambda}, \tag{3}$$

where the Ratio, which uses the IOI described in Eq. (2), is the fraction of photons from the selected spectrum to the total photons detected by the spectrometer.

2.3. Combinatorial growth

The idea for 'combinatorial growth' is from combinatorial chemistry, a branch of chemistry concerned with the synthesis of compounds by combining a number of starting compounds in a variety of ways to build up a large number of product compounds. Using combinatorial growth, we can determine the maximum thickness grown under certain conditions of both Ga flux intensity and nitrogen flux intensity in one experiment. Therefore, combinatorial growth of GaN is a suitable way for evaluating the performance of the RF source.

As described in Refs. [5,18], the Ga and N fluxes are not uniformly distributed on the substrate holder in our MBE system, as shown in Fig. 3a. Thus, when the substrate rotation is turned off, we can grow the GaN under various conditions of III/V ratio with non-uniform Ga and N fluxes in a single growth experiment. After such an experiment, the substrate shows interference colors corresponding to the various thicknesses of GaN (Fig. 3b). When Ga flux distribution was kept constant, the distribution of interference color and Ga droplet distribution in a part of Ga excess region corresponded to the intensity distribution of nitrogen flux because the growth rate was controlled by the effective nitrogen flux. Fig. 3c shows the Ga droplet distribution. In Figs. 3a,b critical change of interference color at the stoichiometric condition is marked by white arrows and a dash line. If the Ga flux intensity was maintained constant while the nitrogen flux was increased, the position of the stoichiometric line moved towards right side such as in Figs. 3a,b the positions of the stoichiometry moved at 6 or higher.

From Fig. 3d, the maximum thickness is confirmed at this fluctuation of interference color by the measured thickness using cross-sectional images obtained from FIB.

3. Results and discussion

3.1. The IOI dependence

Fig. 4a shows the IOI of excited nitrogen species under various inlet pressures of nitrogen gas. Fig. 4b shows

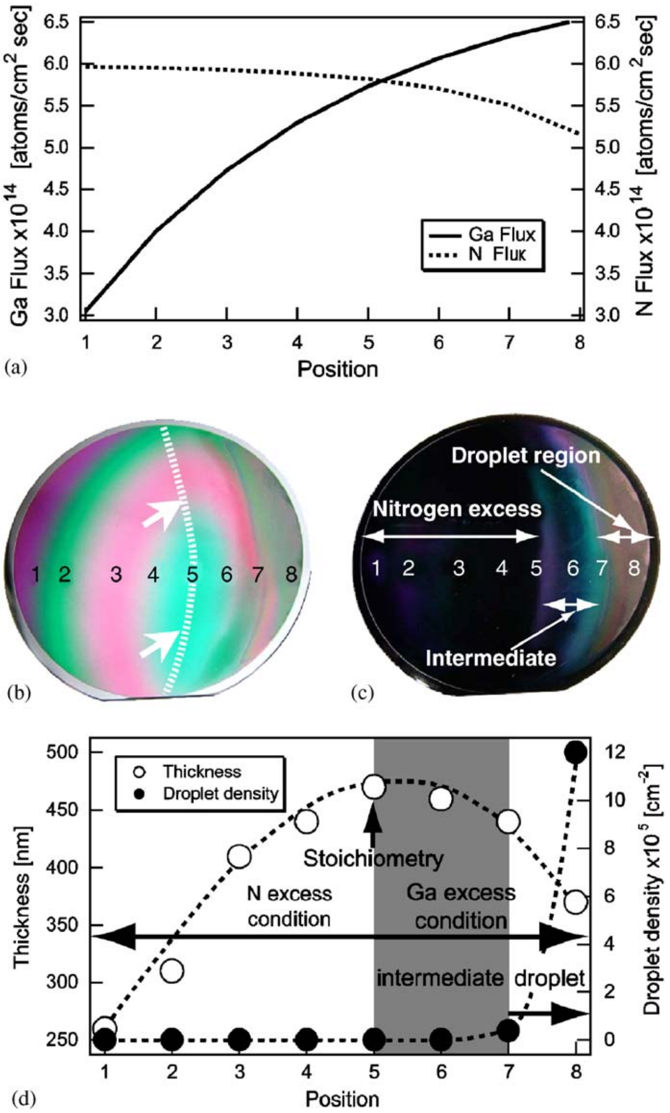

Fig. 3. GaN grown by 'combinatorial growth': (a) distributions of Ga and N flux obtained from Fig. 3(d), (b) interference colors on the sample, (c) illumination of Ga droplet region, (d) distribution of thickness, which were measured from the cross sectional SEM image of the sample, and Ga droplet density.

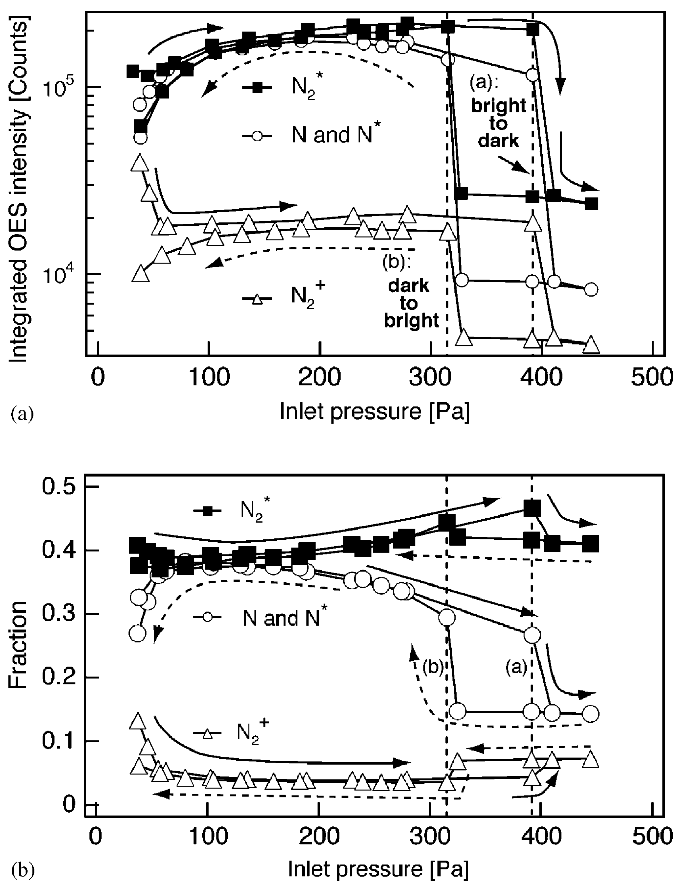

Fig. 4. Relative density and fraction analysis under an RF input power of 400 W: (a) the IOI result, (b) the result of fraction analysis using Eq. (3). Solid arrows show the trend of the increase of inlet pressure and dashed arrows show the trend of the decrease of inlet pressure. The mode shift from bright to dark (indicated as (a)) occurred at 392 Pa whereas that from dark to bright (indicated as (b)) occurred at 315 Pa.

fraction of each particle type calculated by using Eq. (3). The IOIs of N, N^*, and N_2^* were sharply decreased over ~400 Pa where the mode shift of nitrogen plasma from 'bright (B) mode' to 'dark (D) mode' was occured. The B mode shows high IOI, which means active and highly efficient for generation of N and N^*. On the other hand, the D mode produces less N and $N^*$and keep the almost same fraction of N_2^* as shown in Fig. 4b. The summations of the IOI from N and N^* showed a peak-top at around 200 Pa, whereas N_2^* saturated in accordance with the increase of inlet pressure until the discharge mode changed from B to D mode at 392 Pa. The IOI of N_2^+ was not stable at the lower pressure (e.g., 40 Pa). Except for lower inlet pressure, the IOI of N_2^+ showed the saturation until the mode shift from B to D occurred. Then, the inlet pressure was reduced slowly; however, the B mode appeared again at 315 Pa. This 'hysteresis' of the mode change was found in the IOIs of N, N^*, N_2^*, and N_2^+.

3.2. Fraction analysis of nitrogen species

N and N^* are produced in a similar manner as the IOI of N and N^*. However, the fraction of N_2^* for the total IOI was nearly independent of inlet pressure. N_2^+ was effectively produced at 40–50 Pa under dark mode discharge as shown in Fig. 4b. We further confirmed that the condition with a high generation of N and N^* also has a minimal production of N_2^+.

3.3. Combined IOI measurement and fraction analysis

At the low inlet pressure of about 40–50 Pa, free electrons can be gained enough energy by RF electric field because the density of N_2 is small; therefore, the mean free path is large. N_2^* is easily excited and ionized by fast electrons in the plasma. Hence, the ratio of N_2^+ is relatively high at 40–50 Pa. In keeping with the increase of inlet pressure, the dissociated N_2 also increases and thus the IOI of N and N* increase. However, the mean free path is not large enough to accelerate the free electrons according to the increase of inlet pressure. The production of N and N* was not done effectively, thus it gradually reduced the IOI and the fraction of N and N*. On the other hand, the population of N_2^* continuously increased during the IOI measurement because of large amount of N_2 molecules. Excited nitrogen molecules N_2^*, of which state is the $A^3\Sigma_u^+$ state ($N_2^*(A^3\Sigma_u^+)$), have a very long lifetime of ~1 s [19]. According to the following reactions, $N_2^*(A^3\Sigma_u^+)$ would be created from the ground ^{4}S state of nitrogen atom (N (^{4}S)) at the higher inlet pressure according to

$$\begin{aligned} N(^4S) + N(^4S) + M &\rightarrow N_2^*(^3\Sigma_g^+) + M \\ &\rightarrow N_2^*(B^3\Sigma_g,\ v\neq 0) \\ &\rightarrow N_2^*(A^3\Sigma_u^+) + h\nu, \end{aligned} \quad (4)$$

where M is the third body and $h\nu$ corresponds to the emission from the 1st positive series of N_2^*. Thus, the production of N_2^* increased (until the mode shift occurred) due to the recombination of N and the lack of dissociation energy for N_2 and N_2^*.

3.4. Results from IOI and combinatorial growth of GaN

The IOIs of N, N*, and N_2^* are responsible for densities. As shown previously, the plasma discharge under 200 Pa provided a greater number density of N and N* compared to that under 350 Pa. However, the more excited species including N_2^* were obtained at under 350 Pa (Fig. 5) Thus, the IOI of N_2^* should be taken into account for effective species of the GaN growth; the IOI and fraction of N_2^* were increased until the mode shift occurred. $N_2^*(A^3\Sigma_u^+)$ has a very long lifetime and enough activated energy to form GaN [20]. Hence, the increase of thickness in Fig. 5 was caused by the contribution of $N_2^*(A^3\Sigma_u^+)$ to the RF–MBE growth of GaN.

The signal of an optical emission diode (OED) that is used widely in the RF–MBE growth of group-III nitrides [21] must be proportional to the total IOI. As Foxon et al. [21] mentioned that the signal of OED is actually proportional to the total amount of excited nitrogen species. However, the OED signal is not a measure of the amount of N and N* because the contribution of N_2^* to the growth mechanism of group-III nitrides, mainly N_2^* is $N_2^*(A^3\Sigma_u^+)$, is not negligible. If an optical filter for OED is used to obtain only line spectra coming from N and N*, the growth does not always follow the OED signal.

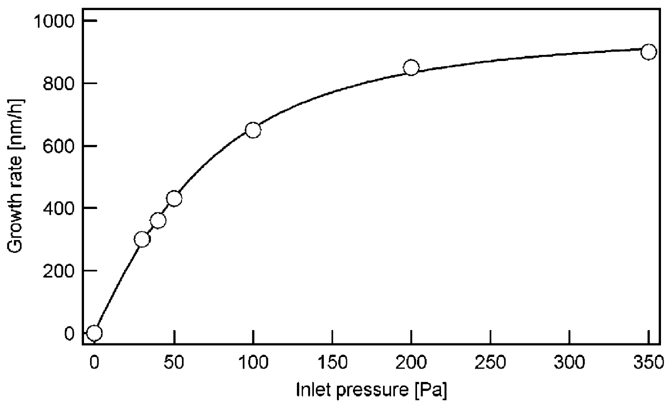

Fig. 5. The inlet pressures dependence of the thickness change of GaN films grown by 'combinatorial growth'.

4. Conclusion

The IOI measurement and fraction of content in the nitrogen plasma discharge was performed under a varying inlet pressure of nitrogen using a nitrogen plasma RF source. At 40–60 Pa for inlet pressure, the production of N_2^+ was relatively high. According to the increase of inlet pressure, the production of N, N*, and N_2^* increased; however, the production of N and N* had a maximum unlike that of N_2^* (until the mode shift occurred). This was due to the lack of energy to dissociate N_2 and N_2^* into N and N*.

Using the combinatorial growth method for GaN and the IOI measurements, the role of excited nitrogen species in the RF–MBE growth was explained. It was shown that the (excited) N* and N_2^* contributed to the growth of GaN. This N_2^* is the long-lived $A^3\Sigma_u^+$ nitrogen molecule.

There is an optimum inlet pressure in the RF–MBE growth of GaN. That is, from the viewpoint of the growth rate, higher inlet pressure is surely better as long as the bright mode discharge and the increase of IOI continue. However, taking into consideration of the pressure of the growth chamber, the stability of MBE machine and the mean free path of excited nitrogen species, an optimum inlet pressure exists.

Acknowledgments

This work was supported by the project, 'Hybrid Nanostructured Materials and Their Application' at the Research Centre for Advanced Science and Technology (RCAST) of Doshisha University. We are also grateful for the contributions from students in our laboratories.

References

[1] R.P. Vaudo, J.W. Kook Jr., J.F. Schetzina, J. Vac. Sci. Technol. B 12 (1994) 1232.
[2] A.J. Ptak, M.R. Millecchia, T.H. Myers, K.S. Ziemer, C.D. Stinespring, Appl. Phys. Lett. 74 (1999) 3836.
[3] A.V. Blant, O.H. Hughes, T.S. Cheng, S.V. Novikov, C.T. Foxon, Plasma Sources Sci. Technol. 9 (2000) 12.
[4] T. Ohachi, T. Kikuchi, K. Miyauchi, Y. Ito, R. Takagi, M. Hogiri, K. Fujita, O. Ariyada, M. Wada, J. Crystal Growth 275 (2005) e1197.
[5] M.J. Paisley, Z. Sitar, J.B. Posthill, R.F. Davis, J. Vac. Sci. Technol. A 7 (1989) 701.
[6] R.W. McCullough, J. Geddes, J.A. Croucher, J.M. Woolsey, D.P. Higgins, M. Schlapp, H.B. Gilbody, J. Vac. Sci. Technol. A 14 (1996) 152.
[7] T. Ohachi, T. Kikuchi, Y. Ito, R. Takagi, M. Hogiri, K. Miyauchi, M. Wada, Y. Ohnishi, K. Fujita, Phys. Stat. Sol. (C) 0 (2003) 2589.

[8] W.C. Hughes, W.H. Rowland Jr., M.A.L. Johnson, S. Fujita, J.W. Cook Jr., J.F. Schetzina, J. Ren, J.A. Edmond, J. Vac. Sci. Technol. B 13 (1995) 1571.
[9] T.D. Moustakas, Mater. Res. Soc. Symp. Proc. 395 (1995) 111.
[10] A. Anders, N. Newman, M. Rubin, M. Dickinson, E. Jones, P. Phatak, A. Gassmann, Rev. Sci. Instrum. 67 (1996) 905.
[11] W.C. Hughes, W.H. Rowland Jr., M.A.L. Johnson, S. Fujita, J.W. Cook Jr., J.F. Schetzina, J. Ren, J.A. Edmond, J. Vac. Sci. Technol. B 13 (1995) 1571.
[12] D. Sugihara, A. Kikuchi, K. Kusakabe, S. Nakamura, Y. Toyoura, T. Yamada, K. Kishino, Phys. Stat. Sol. A 176 (1999) 323.
[13] A.S. Berezhnoi, in: Silicon and its binary systems: Translated from the Russian, Consultants Bureau, New York, 1960. p. 66.
[14] S. Ino, Jpn. J. Appl. Phys. 16 (1977) 891.
[15] N. Osakabe, Y. Tanishiro, K. Yagi, G. Honjo, Surf. Sci. 109 (1981) 353.
[16] Yu. Ralchenko et al., in: National Institute of Standards and Technology (NIST) Atomic Spectra Database, http://physics.nist.gov/PhysRefData/ASD/index.html.
[17] A. Lofthus, P.H. Krupenie, J. Phys. Chem. Ref. Data 6 (1977) 113.
[18] L.W. Sung, H.H. Lin, C.T. Chia, J. Crystal Growth 241 (2002) 320.
[19] D.E. Shemansky, N. Carleton, J. Chem. Phys. 51 (1969) 682; D.E. Shemansky, J. Chem. Phys. 51 (1969) 689.
[20] N. Newman, J. Crystal Growth 178 (1997) 102.
[21] C.T. Foxon, I. Harrison, S.V. Novikov, A.J. Winser, R.P. Campion, T. Li, J. Phys.: Condens. Matter. 14 (2002) 3383.